

Evaluation of Cubic-Spline Based Gas Kinetic Method for Simulating Compressible Turbulence

N. Parashar^{1†}, B. Srinivasan² and S. S. Sinha¹

¹ Department of Applied Mechanics, Indian Institute of Technology Delhi, New Delhi 110016, India

² Department of Mechanical Engineering, Indian Institute of Technology Madras, Chennai 600036, India

†Corresponding Author Email: nishantparashar14@gmail.com

(Received September 25, 2018; accepted January 20, 2019)

ABSTRACT

In this work, we implement and examine a new flow reconstruction methodology using cubic-splines for interpolations in the gas kinetic method (GKM). We compare this version of GKM with the existing WENO based interpolation method. The comparisons are made in terms of accuracy and computational speed. We find that at low to intermediate range of Mach number ($M_t < 0.7$), cubic-splines based interpolations are superior in terms of reduced numerical dissipation and higher computational speed (7x faster) as compared to the WENO interpolation method.

Keywords: Compressible flows; Gas kinetic method; Direct numerical simulation; Turbulence; Decaying isotropic flow.

NOMENCLATURE

M_t	Turbulent Mach number	K_T	thermal conductivity
Re_λ	Taylor Reynolds number	\mathbf{V}	velocity of fluid
μ	fluid viscosity	T	temperature
ν	kinematic viscosity	ρ	density
k	turbulent kinetic energy	P	pressure
K	boltzmann constant	τ	large eddy turnover time
ε	dissipation rate	\dot{q}	heat flux
θ	divergence	σ_{nn}	normal Stress
\overline{F}	velocity derivative flatness (kurtosis)	\overline{I}_t	average iteration time

1. INTRODUCTION

Direct numerical simulation (DNS) of turbulent flow has improved our understanding of many fundamental aspects of turbulence (Honein and Moin (2004), Kerimo and Girimaji (2007), Cambon *et al.* (1993), Sarkar *et al.* (1991)). Data from the DNS simulations has led to the development of better turbulence closure models as well (Sarkar *et al.* (1991), Girimaji and Speziale (1995)). For incompressible flows, there is a range of higher-order methods that have been established for performing DNS of turbulent flows. However, direct numerical simulation of compressible turbulence poses greater challenges due to the appearance of shocks in a turbulent flow field. During the last two decades, various numerical schemes have been

developed that can efficiently simulate compressible turbulence (Passot and Pouquet (1987), Samtaney *et al.* (2001), Sandham *et al.* (2002), Honein and Moin (2004), Martin *et al.* (2006), Kumar *et al.* (2013), etc.]. However, all these numerical schemes have been shown to simulate compressible turbulent flows for a limited range of operation in terms of Mach number and Reynolds number.

In recent years, the gas kinetic method (GKM) proposed by Xu (2001) has evolved as a robust method for simulating compressible turbulent flows. The gas-kinetic BGK method (GKM) has various advantages over the conventional Navier-Stokes (NS) based solvers due to its robustness over a wide range of turbulent Mach number and its ability to accurately capture flow physics. Furthermore, the GKM scheme is also capable of

capturing deviations from equilibrium and effect of extremely rarefied flow physics (Ragta *et al.* (2017b), Ragta *et al.* (2017a)).

Navier-Stokes equation can be extracted from the BGK model (Bhatnagar *et al.* (1954)) by applying the Chapman-Enskog expansion. However, the BGK model constraints the Prandtl number to unity. Prandtl number corrections were later developed by Xu (1998) and May *et al.* (2007). The BGK gas-kinetic scheme was for the first time employed for simulating weakly compressible turbulence by Kerimo and Girimaji (2007) at a Mach number of 0.052. Later, Liao *et al.* (2009) and Parashar *et al.* (2017) employed different variants of the GKM scheme using continuous flow reconstruction to simulate compressible turbulent flows for turbulent Mach numbers up to 0.5. Kumar *et al.* (2013) enhanced the GKM scheme (Xu *et al.* (2005)) with weighted essentially non-oscillatory method (WENO, Liu *et al.* (1994)) for discontinuous flow reconstruction to simulate compressible turbulent flows at high turbulent Mach number of 1.75.

While simulating compressible turbulent flows using GKM, a transition from continuous flow reconstruction at low Mach number to discontinuous reconstruction at high Mach number has to be made. While continuous flow reconstruction has been shown to accurately capture flow physics for turbulent Mach number up to 0.5 (Liao *et al.* (2009), Parashar *et al.* (2017)), discontinuous reconstruction using WENO has been shown to accurately simulate highly compressible flow at higher Mach numbers. Liao *et al.* (2009), showed that the use of discontinuous reconstruction with limiters produces excessive numerical dissipation in the flow field. The use of WENO based methods for discontinuous flow reconstruction has been shown to reduce the numerical dissipation for turbulent flows at high turbulent Mach number ($M_t > 1$) by Kumar *et al.* (2013). However, the validation of GKM with WENO based interpolations (against established higher order accurate Navier Stokes based solutions) has not been performed for low and moderate range of Mach numbers (Kumar *et al.*, 2013). Thus there is a scope of development of better reconstruction methods for GKM, especially at low and moderate Mach numbers. In this work, we introduce a new interpolation methodology using cubic-spline based continuous flow reconstruction and determine its range of applicability for simulating compressible turbulent flows.

The prime objective of this work is to propose a new flow reconstruction methodology with GKM which uses cubic spline based interpolation. This new flow reconstruction methodology is extensively evaluated over a range of Mach and Reynolds number. Comparisons of the new methodology are made against WENO based interpolations with GKM. We first perform comparisons for one-dimensional normal shock structure. Subsequently, we make comparisons for three-dimensional decaying isotropic turbulence. Our results are also compared with high order accurate Navier-Stokes based results of Samtaney *et al.* (2001).

This paper is organized into 5 sections. In section 2, we present the governing equations and a brief

review of the gas kinetic method (GKM). In section 3 we present our novel cubic-spline based reconstruction method. In section 4 we present our plan of systematically evaluating the cubic-spline reconstruction based GKM. Numerical results and discussions are shown in section 5. We conclude our work with a summary in section 6.

2. GOVERNING EQUATIONS

The governing equations of compressible flow field of a perfect gas are the continuity, momentum, energy and state equation:

$$\frac{\partial \rho}{\partial t} + V_k \frac{\partial \rho}{\partial x_k} = -\rho \frac{\partial V_k}{\partial x_k}, \quad (1)$$

$$\frac{\partial V_i}{\partial t} + V_k \frac{\partial V_i}{\partial x_k} = -\frac{1}{\rho} \frac{\partial p}{\partial x_i} + \frac{1}{\rho} \frac{\partial \sigma_{ik}}{\partial x_k}, \quad (2)$$

$$\begin{aligned} \frac{\partial T}{\partial t} + V_k \frac{\partial T}{\partial x_k} = & -T(n-1) \frac{\partial V_i}{\partial x_i} - \frac{n-1}{\rho R} \frac{\partial q_k}{\partial x_k} \\ & + \frac{n-1}{\rho R} \frac{\partial}{\partial x_j} (V_i \sigma_{ji}), \end{aligned} \quad (3)$$

$$p = \rho RT, \quad (4)$$

where V_i , x_i , ρ , p , T , R , σ_{ik} , q_k , n denote velocity, position, density, pressure, temperature, gas constant, stress tensor, heat flux and ratio of specific heat values, respectively. The quantities σ_{ij} and q_k obey the following constitutive relationships:

$$\sigma_{ij} \equiv \mu \left(\frac{\partial V_i}{\partial x_j} + \frac{\partial V_j}{\partial x_i} \right) + \delta_{ij} \lambda_\mu \frac{\partial V_k}{\partial x_k}, \quad \text{and} \quad (5)$$

$$q_k \equiv -K_T \frac{\partial T}{\partial x_k}, \quad (6)$$

where δ_{ij} is the Kronecker delta, K_T represents the thermal conductivity, and μ and λ_μ ($\lambda_\mu = -\frac{2\mu}{3}$) denote the first and second coefficients of viscosity respectively.

2.1 Finite Volume Gas Kinetic Scheme (GKM)

Any general finite volume scheme for solving Navier-Stokes equation updates the conservative flow field, W (from n^{th} to $n+1^{\text{th}}$ time step), using the following evolution equation:

$$\begin{aligned} W_{i,j,k}^{n+1} - W_{i,j,k}^n = & \frac{1}{dx} \int (F_{i-1/2,j,k}(t) - F_{i+1/2,j,k}(t)) dt \\ & + \frac{1}{dy} \int (F_{i,j-1/2,k}(t) - F_{i,j+1/2,k}(t)) dt \\ & + \frac{1}{dz} \int (F_{i,j,k-1/2}(t) - F_{i,j,k+1/2}(t)) dt; \end{aligned} \quad (7)$$

where F is the flux calculated at the cell interface,

bounding the cell at the grid point, (i, j, k) . The conservative macroscopic fluid variable (W) is defined as:

$$W = \begin{pmatrix} \rho \\ \rho V_x \\ \rho V_y \\ \rho V_z \\ \rho e \end{pmatrix} \quad (8)$$

where ρ is the macroscopic fluid density, V_x, V_y, V_z are the three components of the fluid velocity \mathbf{V} and e is the specific internal energy. In finite volume GKM, the flux is evaluated using the kinetic theory, where the governing equation for the evolution of the particle distribution function is the Boltzmann equation:

$$f_t + uf_x + vf_y + wf_z = Q; \quad (9)$$

where u, v, w are the components of internal particle velocity and Q is the collision term. In finite volume gas kinetic scheme, the Bhatnager-Gross-Krook (BGK) approximation for the Boltzmann equation is used for flux calculation. The BGK equation (Bhatnagar *et al.* 1954) in three-dimension is given by:

$$f_t + uf_x + vf_y + wf_z = \frac{g - f}{Tc}; \quad (10)$$

where f is the gas distribution function, Tc is the collision time scale and g is the equilibrium distribution function taken to be the Maxwellian:

$$g = \rho \left(\frac{\Lambda}{\pi} \right)^{\frac{N+3}{2}} e^{-\lambda[(u-V_x)^2 + (v-V_y)^2 + (w-V_z)^2 + \xi_1^2 + \xi_2^2 + \dots + \xi_N^2]} \quad (11)$$

where ρ is the density, N is the number of degrees of freedom, ξ is internal flow variable and Boltzmann constant (K) is related to the gas temperature (T) and molecular mass (m) as, $\Lambda = m/2KT$.

In equilibrium state:

$$\xi^2 = \xi_1^2 + \xi_2^2 + \dots + \xi_N^2. \quad (12)$$

The macroscopic conservative variables are related to the gas distribution function as:

$$W = \int \psi f du dv dw d\xi; \quad (13)$$

where ψ is defined as:

$$\psi = \begin{pmatrix} 1 \\ u \\ v \\ w \\ \frac{1}{2}(u^2 + v^2 + w^2 + \xi^2) \end{pmatrix} \quad (14)$$

The flux in x-direction can be calculated by taking the moment of the distribution function:

$$F_x(W) = \begin{pmatrix} F_\rho \\ F_{\rho V_x} \\ F_{\rho V_y} \\ F_{\rho V_z} \\ F_{\rho e} \end{pmatrix} = \int \psi f du dv dw d\xi; \quad (15)$$

Similarly, flux in other directions (y and z) can also be calculated. Integrating the BGK Equation (10), from $x \in (x_{i-1/2}, x_{i+1/2})$, $y \in (y_{j-1/2}, y_{j+1/2})$, $z \in (z_{k-1/2}, z_{k+1/2})$ & $t \in (t^n, t^{n+1})$ we get:

$$\int (f_t + uf_x + vf_y + wf_z) \psi du dv dw d\xi dx dy dz dt = \int \frac{g - f}{Tc} \psi du dv dw d\xi dx dy dz dt. \quad (16)$$

Rearranging the terms in Eq. (16), we obtain Eq. (7). The flux F , is calculated using the BGK model (Eq. 10). The instantaneous distribution function f at the cell interface $(x_{i+1/2}, y_j, z_k)$ is obtained using the general solution of the BGK model at a cell interface $(x_{i+1/2}, y_j, z_k)$ and time t :

$$f(x_{i+1/2}, y_j, z_k, t, u, v, w, \xi) = \frac{1}{Tc} \int_0^t g(x', y', z', t', u, v, w', \xi) e^{-t'/Tc} f_0(x_{j+1/2} - ut, y_j - vt, z_k - wt); \quad (17)$$

where $x' = x_{i+1/2} - u(t - t')$, $y' = y_j - v(t - t')$, $z' = z_k - w(t - t')$ represents the trajectory of a particle motion and f_0 is the initial gas distribution function at the beginning of each time step ($t = 0$). The reader is referred to [Xu *et al.* \(2005\)](#) for the full description of the gas kinetic method.

2.2 Cubic-spline based reconstruction method

In finite volume method, the flow field is updated at each time step at the computational nodes, which are the centres of computational cells in the discretized flow-field. In order to find the flux at the cell interface using any finite volume method based numerical scheme, the flow variables need to be approximated at the cell interface. For this, the flow information at the computational nodes is used to reconstruct the flow field at the cell interface using a suitable interpolation methodology. [Kumar *et al.* \(2013\)](#) have earlier used WENO based interpolation scheme—especially for high Mach number flows. The reader is referred to [Kumar *et al.* \(2013\)](#) for further details on the WENO-based reconstruction scheme. In this work, we introduce a new flow reconstruction methodology with GKM using cubic-splines for flow reconstruction. The details of cubic spline based interpolation are presented in the following sub-section.

3 CUBIC-SPLINE BASED FLOW RECONSTRUCTION

Splines are piecewise polynomial functions of the form:

$$F(x) = \begin{cases} f_1(x), & \text{if } x_1 \leq x < x_2 \\ f_2(x), & \text{if } x_2 \leq x < x_3 \\ \vdots & \vdots \\ f_{n-1}(x), & \text{if } x_{n-1} \leq x < x_n \end{cases} \quad (18)$$

where x is the position of the node, n is the total number of nodes in the domain and f_i is a cubic polynomial defined as:

$$f_i(x) = a_i + b_i(x - x_i) - c_i(x - x_i)^2 + d_i(x - x_i)^3. \quad (19)$$

For finding these four coefficients per piecewise function, we need four equations:

1. The function value at the node is known: $f_i(x_i) = y_i$.
2. $F(x)$ should be continuous: $f_i(x_{i+1}) = f_{i+1}(x_i)$.
3. First derivative of $F(x)$ should be continuous:

$$\frac{df_i(x_{i+1})}{dx} = \frac{df_{i+1}(x_i)}{dx}$$

4. Second derivative of $F(x)$ should be continuous:

$$\frac{d^2 f_i(x_{i+1})}{dx^2} = \frac{d^2 f_{i+1}(x_i)}{dx^2}$$

For the first and the last spline, the derivative information is not available. Hence, certain boundary conditions need to be imposed at the ends to close the $4(n - 1)$ set of algebraic equations. In this work, we have used natural boundary condition for one-dimensional normal shock problem, setting the second derivative to zero at the boundary. For three-dimensional isotropic turbulence simulations we have used periodic boundary conditions wherein the first and second derivative at the opposite boundary ends are kept equal. The interpolation methodology for one-dimensional cubic-splines is extended for multi-dimensions as well. The reader is referred to Habermann and Kindermann (2007) for further details on the multi-dimensional cubic-spline interpolation method.

The open source library Einspline (Esler, 2007) has been used for finding cubic splines in the present work. We use such cubic-spline based flow reconstructions to find flow variables and their derivatives at the cell interface using Eq. (17).

4. PLAN OF STUDY

We first test cubic splines based reconstruction with GKM for one-dimensional normal shock problem in section 5.1. In viscous flow, shock has a viscosity and Mach number dependent structure (Xu, 2001). We incorporate cubic splines with GKM to capture this shock structure and compare our findings against Navier-Stokes based solution.

While doing so we also compare our results against WENO based interpolations. These comparisons are performed for Mach numbers of 1.5, 5 and 7. Comparisons are performed in terms of flow variables: velocity (U) and Temperature (T); and the derived non-dimensional quantities: heat flux (\dot{q}) and normal stress (σ_{nn}), which are defined as:

$$\dot{q} = -\frac{5}{4} \frac{\mu}{p} \frac{dT}{Pr dx}; \quad \sigma_{nn} = \frac{2\mu}{3p} \frac{dU}{dx}; \quad (20)$$

where p is pressure, μ is the kinematic viscosity, Pr is the Prandtl number and c is the acoustic speed. The initial state of the shock problem are:

1. Upstream state $-\infty < x \leq 0$: $\rho_l = 1, U_l = 1$
2. Downstream state $0 < x < \infty$:

$$\rho_r = \frac{(\gamma + 1)M^2}{(2 + (\gamma - 1)M^2)} \rho_l,$$

$$U_r = \left(\frac{(\gamma - 1)}{(\gamma + 1)} + \frac{2}{(\gamma + 1)/M^2} \right) U_l$$

where $\gamma = 5/3$ is the specific heat ratio, fluid Prandtl number $Pr = 1$, viscosity $\mu = 0.0005$. The computational domain is $-1.0 \leq x \leq 1.0$, grid size $dx = 0.0013$ and number of computational nodes $n = 1500$. Natural boundary condition is applied at the end points.

In section 5b we perform the direct numerical simulation of decaying isotropic turbulence using the new cubic-spline based flow reconstruction methodology. The DNS results obtained using cubic-spline flow reconstruction (with GKM) are compared with established Navier-Stokes based DNS results of Samtaney *et al.* (2001). DNS results using GKM with WENO based flow reconstruction are also shown in this section. Direct numerical simulations of decaying isotropic turbulence are performed over a cubic domain with 2π as the edge length. The boundary conditions are periodic and the initial velocity field is constrained to have zero mean and the following energy spectrum:

$$E(\kappa) = A \kappa^4 \exp(-2\kappa^2 / \kappa_0^2); \quad (21)$$

where, A is a spectrum constant and κ represents wavenumber, with κ_0 being the value of κ corresponding to the peak of the energy spectrum. The initial thermodynamic properties are kept constant and fluctuation free. M_t is the turbulent Mach number defined as:

$$M_t = \sqrt{\frac{2k}{\gamma R \bar{T}}}; \quad (22)$$

where \bar{T} is the mean temperature, R is the gas constant, γ is specific heat ratio and k is the turbulent kinetic energy ($k = \frac{1}{2} V_i' V_i'$) with V_i' being the fluctuating velocity field. Note that an overbar indicates mean value. The relevant Reynolds number is the Taylor's Reynolds number defined as:

Table 1 Initial parameters of DNS simulations

Sim.	low $Re_\lambda = 72$	Sim.	high $Re_\lambda = 175$
A	$M_t = 0.3, grid = 128^3$	B	$M_t = 0.3, grid = 256^3$
C	$M_t = 0.5, grid = 128^3$	D	$M_t = 0.488, grid = 256^3$
E	$M_t = 0.7, grid = 128^3$	F	$M_t = 0.7, grid = 256^3$

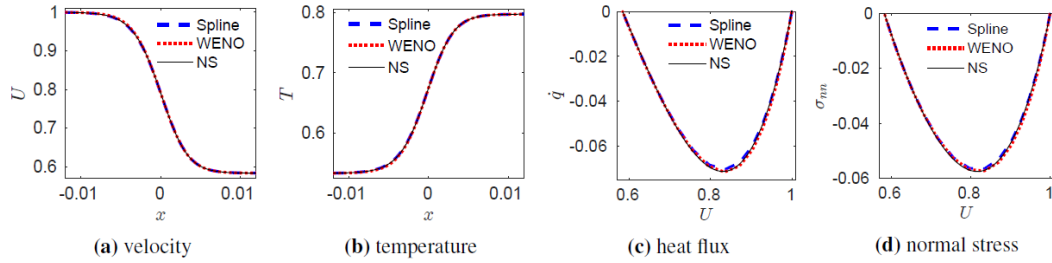


Fig. 1. Results for normal shock structure $M = 1.5$.

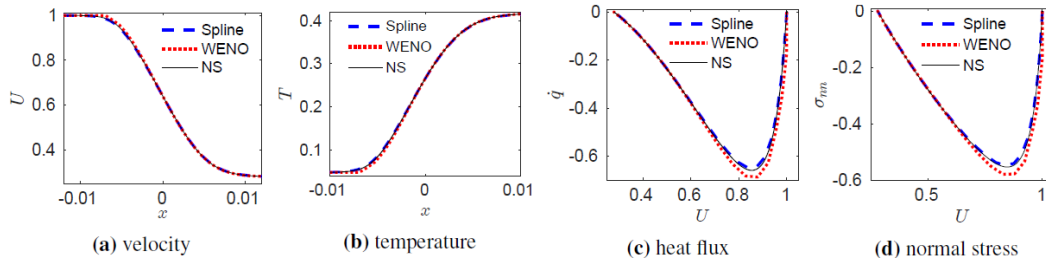


Fig. 2. Results for normal shock structure $M = 5$.

$$Re_\lambda = \sqrt{\frac{20}{3\varepsilon\nu}}k; \quad (23)$$

where ε , ν are dissipation-rate and kinematic viscosity respectively and λ is the Taylor microscale. Fluid Prandtl number $Pr = 0.7$ and specific heat ratio $\gamma = 1.4$ (for air) is chosen for all the simulations. In total six simulations of decaying isotropic turbulence are performed for this study as mentioned in Table 1.

Comparisons are made in terms of turbulent kinetic energy (k) and divergence $\left(\theta = \frac{1}{3} \sqrt{\left(\frac{\partial V'_i}{\partial x'_i} \right)^2} \right)$.

The time has been normalized using τ , which represents the eddy turnover time (Yeung and Pope (1989), Elghobashi and Truesdell (1992), Samtaney *et al.* (2001), Martín *et al.* (2006)):

$$\tau = \frac{L_0}{V_{rms}} \quad (24)$$

where V_{rms} is the root mean square (rms) velocity and L_0 is the integral-length-scale of the initial flow field (at time, $t = 0$). Extensive comparison between cubic-spline and WENO for a range of Mach number and Reynolds number (Table 1) are presented in sections 5.2.1–5.2.4.

In section 5c, we investigate the computational speed of GKM with spline-based reconstruction. Computational speed of spline-based reconstructions

is compared with WENO based reconstruction. This comparison is made in terms of total time for the completion of simulation from $t = 0$ to $t = 8\tau$.

5. RESULTS

In this section, we show results of one-dimensional shock structure followed by direct numerical simulation of decaying compressible isotropic turbulence using GKM with cubic-spline based interpolation methodology. In section 5a we show the performance of cubic-spline based interpolations in capturing the shock structure. In section 5.2, we show DNS results of decaying isotropic turbulence using GKM with cubic-spline based flow reconstruction against WENO based flow reconstruction and benchmark results of Samtaney *et al.* (2001). We, further evaluate the computational accuracy of cubic-spline based flow reconstruction over a range of turbulent Mach and Reynolds number (Table 1) in sections (5.2.1–5.2.6). Finally in section 5.3, we compare the computational speed of GKM with cubic-spline based flow reconstruction against WENO based flow reconstruction method.

5.1 Normal shock structure

In Figs. 1(a), 2(a) and 3(a) we show velocity profiles for three Mach number of 1.5, 5 and 7 respectively. Similarly Figs 1–3(b) temperature profile is plotted. It can be observed that cubic-spline based flow reconstruction perfectly captures the velocity and temperature profile. The deviations

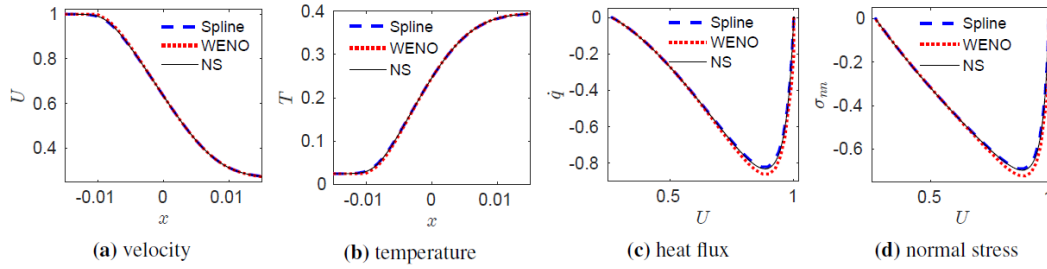


Fig. 3. Results for normal shock structure $M = 7$.

Table 2 Maximum error (L_∞ norm) in flow variables for normal shock problem

		U	p	T	ρ
$M = 1.5$	spline	1.998e-3	5.093e-4	3.326e-3	5.873e-3
	WENO	2.435e-3	1.560e-3	3.442e-3	6.003e-3
$M = 5$	spline	1.079e-4	9.200e-4	7.803e-4	1.969e-3
	WENO	4.347e-3	4.048e-3	7.257e-3	1.840e-2
$M = 7$	spline	9.099e-4	1.289e-3	6.447e-4	2.507e-3
	WENO	8.795e-3	5.474e-3	4.537e-3	2.399e-2

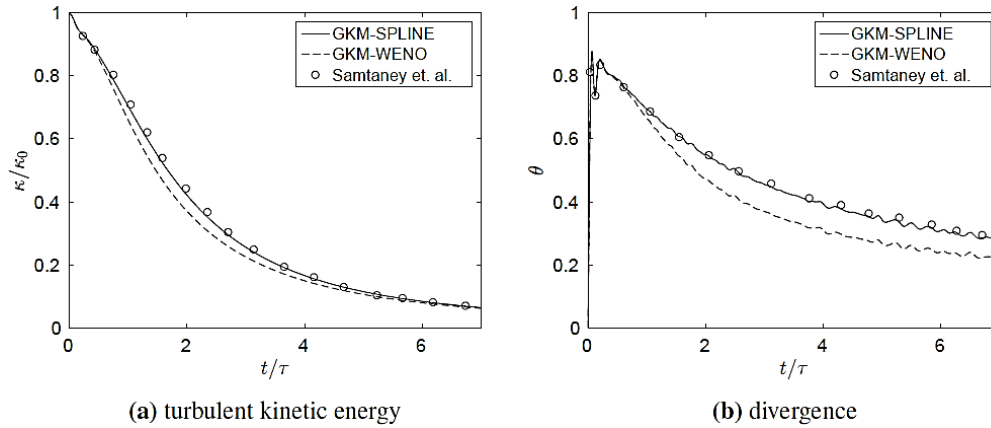


Fig. 4. Comparison of DNS results for Simulation A.

from accurate Navier-Stokes based solution (Xu, 2001) are found to be negligible. Further, we find that cubic-spline based interpolation performs better than WENO based interpolations, especially in the upstream region ($x \approx -0.01$).

In Table 2 we show maximum error in each flow variable for both spline and WENO based reconstruction methods. It is evident from Table 2 that spline based flow reconstruction method has better accuracy as compared to WENO at all Mach numbers. Further, we plot derived flow quantities viz. heat flux q and normal stress σ_{nn} with velocity in Figs. 1–3(c) and 1–3(d) respectively. It can be seen in Figs. 1–3(c) and 1–3(d) that while cubic-spline shows an almost perfect match with the Navier Stokes solution, WENO based interpolations overestimates the heat-flux and normal stress. Hence, we conclude that cubic-spline based flow reconstruction with GKM is capable of accurately capturing discontinuities and is in fact found to be more accurate compared to WENO.

5.2 DNS of decaying isotropic turbulence

In this section, we show DNS results of GKM using cubic-spline based flow reconstruction. DNS results of GKM with cubic spline based reconstruction are compared against WENO based reconstruction method. Navier Stokes based DNS results of Samtaney *et al.* (2001) are used as a benchmark for comparing the two interpolation schemes.

5.2.1 Low M_t , low Re_λ

In this section, we show the turbulence statistics obtained from DNS of decaying isotropic turbulence using GKM with cubic-spline based reconstruction for low turbulent Mach number and low Reynolds number (Simulation A, Table 1). The results are compared against GKM with WENO based flow reconstruction. In Figs. 4(a) and 4(b), we show evolution of turbulent kinetic energy (k) and divergence (θ) respectively for Simulation A. Results of Samtaney *et al.* (2001) are also shown in these figures (Figs. 4(a–b)). It can be observed that cubic

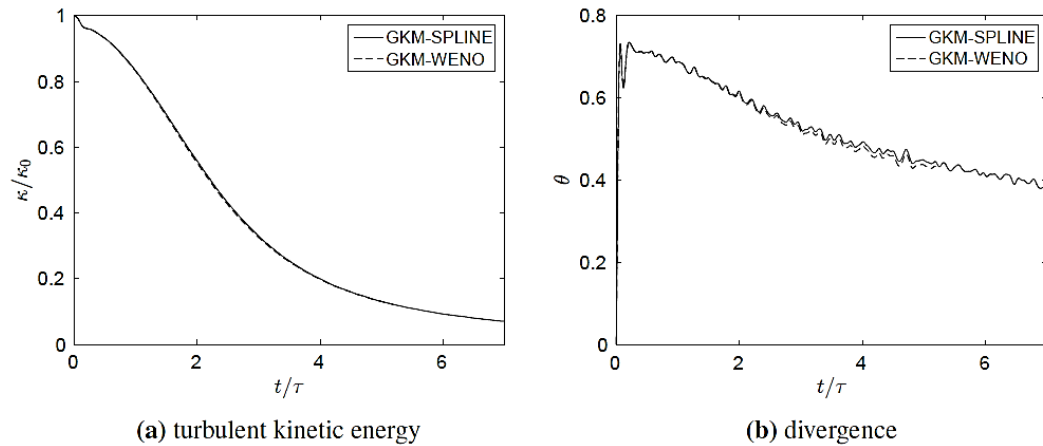


Fig. 5. Comparison of DNS results for Simulation B.

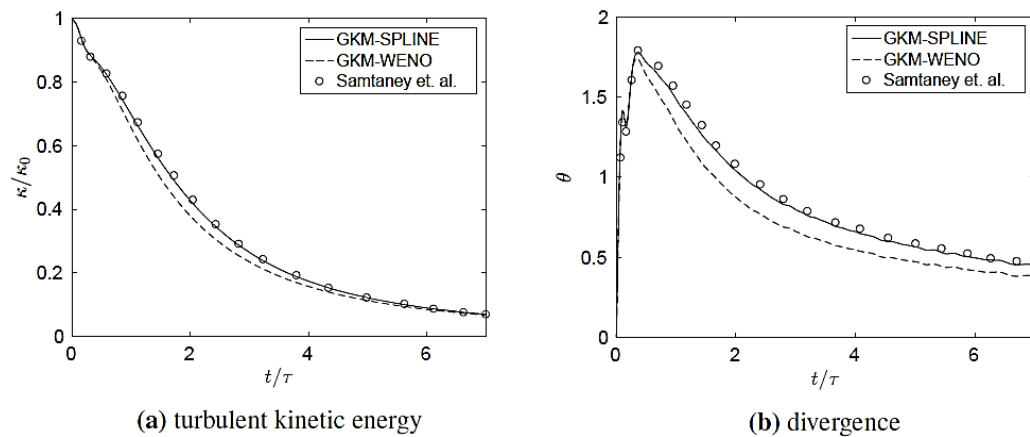


Fig. 6. Comparison of DNS results for Simulation C.

spline based reconstruction method shows good agreement with results of [Samtaney *et al.* \(2001\)](#) (Figs 4a and 4b). On the other hand WENO based flow reconstruction are found to yield numerically dissipative results as compared to cubic-spline based reconstruction.

At low turbulent Mach number, the flow field is relatively smooth and hence the usage of discontinuous flow reconstruction will yield higher numerical dissipation. Due to this reason WENO based flow reconstruction is showing numerically dissipative solution as compared to non-discontinuous spline based flow reconstruction. However, the performance of discontinuous flow reconstruction using WENO is expected to improve with increasing M_t . Based on these results, we conclude that at low Reynolds and Mach numbers, the cubic-spline based flow-reconstruction scheme should be the preferred flow reconstruction methodology compared to the WENO based flow reconstruction method.

5.2.2 Low M_t , high Re_λ

There is no benchmark solution available in this regime (low M_t and high Re_λ , Simulation B). Hence, our comparisons are made directly with the DNS results of GKM using WENO based flow

reconstruction method. In Fig 6, we show evolution of the same turbulent statistics (viz. (a) turbulent kinetic energy, and (b) divergence) as discussed in section 5.2.1. Results from the two schemes seem almost identical in terms of turbulent kinetic energy and divergence.

5.2.3 Moderate M_t , low Re_λ

In Fig. 6 we perform our comparisons at moderate turbulent Mach number and low Reynolds number (Simulation C). Benchmark simulation result of [Samtaney *et al.* \(2001\)](#) are available in this regime and are also shown in Fig. 6. It can be observed that cubic spline based reconstruction method shows good agreement with results of [Samtaney *et al.* \(2001\)](#). WENO based interpolations are found to yield dissipative results as compared to cubic-spline based reconstruction while comparing these turbulent statistics (Fig. 6).

5.2.4 Moderate M_t , high Re_λ

In Fig. 7, we show the different turbulent statistics at moderate turbulent Mach number and high Reynolds number (Simulation D). Benchmark simulation result of [Samtaney *et al.* \(2001\)](#) are also shown in Fig. 7. We observe that both the cubic spline and the WENO based reconstruction methods show good agreement with results of [Samtaney *et al.*](#)

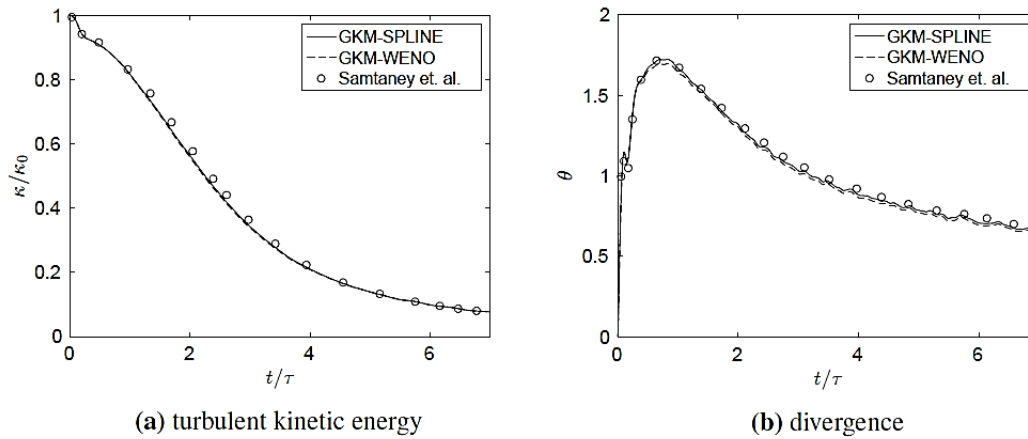


Fig. 7. Comparison of DNS results for Simulation D.

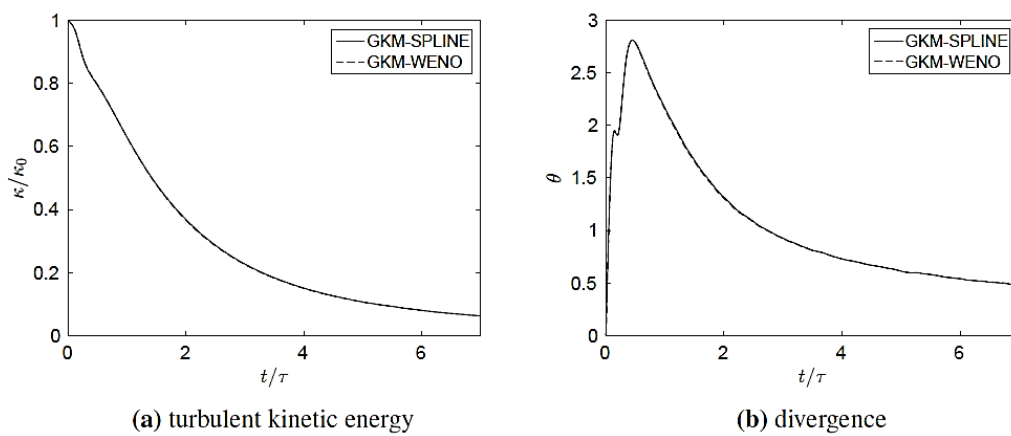


Fig. 8. Comparison of DNS results for Simulation E.

(2001) while comparing k and θ (Figs. 7(a) and 7(b)).

5.2.5 High M_t , low Re_λ

In Fig. 8, we show evolution of different turbulent statistics in high M_t , low Re_λ regime. We observe that both the cubic spline and the WENO based reconstruction methods show almost perfect agreement with each other while comparing both turbulent kinetic energy and divergence (Fig. 8). The results of cubic-spline and WENO based flow reconstruction be-comes identical at this high M_t . Observing the trends of previous simulation results (Simulation A–D), we expect that for $M_t \geq 0.7$, the excess numerical dissipation encountered with WENO based discontinuous flow reconstruction (especially at low Reynolds number) would almost cease to exist.

5.2.6 High M_t , high Re_λ

Cubic-spline based flow reconstruction with GKM is found to be numerically unstable while simulating turbulence at high M_t and high Re_λ . As seen in the previous section (5b6), for high M_t WENO based flow reconstruction yields numerically non-dissipative solutions. Further, we have also shown that while increasing M_t and Re_λ the numerical dissipation of WENO based reconstruction reduce

significantly. Hence, beyond this range of Mach number ($M_t \geq 0.7$) WENO should be the preferred choice for simulating compressible turbulence.

We finally conclude the most efficient interpolation methodology (in terms of accuracy) with GKM for performing DNS of decaying compressible turbulence (between WENO and cubic-spline). In Table 3 we show most suitable interpolation methodology for different combinations of M_t and Re_λ . For low to moderate Mach number ($M_t \leq 0.5$) cubic-spline flow reconstruction is found to yield higher accuracy than WENO based flow reconstruction.

5.3 Computational speed of GKM with cubic spline flow reconstruction

In this section, we present the comparison of computational speed of GKM with cubic-spline based reconstruction method with WENO based reconstruction method. We consider two grids with sizes of 128^3 and 256^3 respectively. Intel processor E5-2680v3 (2.5GHz) is used for finding the simulation time. We also show the computational speeds by performing our tests on two different choices of the number of processors: a) 8 processors and b) 64 processors.

Table 3 Superior choice between cubic-spline and WENO in different flow regimes

	(low) $Re_\lambda = 72$	(high) $Re_\lambda = 175$
$M_t = 0.3$	cubic-spline	both cubic-spline and WENO
$M_t = 0.5$	cubic-spline	both cubic-spline and WENO
$M_t = 0.7$	both cubic-spline and WENO	WENO

Table 4 Speed-up shown by the two schemes

Grid	Processors	T_{spline} (hr)	T_{weno} (hr)	$\frac{T_{weno}}{T_{spline}}$
128^3	8	2.91	19.17	6.6
128^3	64	0.38	2.48	6.5
256^3	8	91.73	669.6	7.3
256^3	64	12.41	88.11	7.1

In Table 3, we show the total time for completing of simulation using cubic-spline (T_{spline}) and WENO based reconstruction methods (T_{weno}). It can be observed that cubic-spline based reconstruction is approximately 7x faster than WENO based flow reconstruction on both the grids as well as both 8 and 64 processors setups. In WENO based flow reconstruction with GKM, two different discontinuous flow states and correspondingly two different distribution functions are generated numerically at the cell interface at each time step. These different flow states makes the flux computation extremely complex. While, in spline reconstruction, only one flow state and distribution function is constructed at the cell interface leading to simpler flux calculations and reduced computational cost. This gives an advantage to cubic-spline over WENO based flow reconstruction in low and moderate Mach number regimes ($M_t \leq 0.5$), where GKM-spline is not only computationally more accurate but computationally cheaper as well (Table 3 and 4). Further, we observe that the computational speed of cubic-spline method shows good scalability with the number of processors.

6. CONCLUSIONS

In this work, we introduce a new interpolation methodology for GKM using cubic-spline for flow-reconstruction/interpolation at the cell interface. Comparison of the cubic-spline based flow reconstruction is made against WENO based flow reconstruction method. We find that cubic-spline based interpolations are capable of accurately capturing the normal shock structure for $M \leq 7$. The performance of cubic-spline flow reconstruction is found to be superior as compared to the WENO reconstruction method in capturing the normal shock structure. Further, we perform the direct numerical simulation of decaying isotropic compressible turbulence over a range of Mach number ($0.3 \leq M_t \leq 0.7$) and two different Reynolds number (72 and 175). We find that for low and moderate values of Mach number and Reynolds numbers the newly

introduced cubic-spline interpolation scheme performs superior as compared to WENO in terms of numerical accuracy. We also find that, as Mach number and Reynolds number increase, results from both cubic-spline and WENO based flow reconstructions show close agreement with each other. Further, the cubic-spline based flow reconstruction method is found to be approximately 7x faster than WENO based flow reconstruction method with GKM.

ACKNOWLEDGMENTS

The authors are thankful to the High Performance Computing (HPC) facility of the Indian Institute of Technology (IIT) Delhi for providing computational resources for this work

REFERENCES

- Bhatnagar, P. L., E. P. Gross and M. Krook (1954). A model for collision processes in gases. i. small amplitude processes in charged and neutral one-component systems. *Physical Review* 94, 511–525.
- Cambon, C., G. N. Coleman and N. N. Mansour (1993). Rapid distortion analysis and direct simulation of compressible homogeneous turbulence at finite Mach number. *Journal of Fluid Mechanics* 257, 641–665.
- Elghobashi, S. and G. C. Truesdell (1992). Directsimulation of particle dispersion in a decaying isotropic turbulence. *Journal of Fluid Mechanics* 242, 655700.
- Esler, K. (2007). Einspline b-spline library. <http://einspline.sourceforge.net/>.
- Girimaji, S. S. and C. G. Speziale (1995). A modified restricted Euler equation for turbulent flows with mean velocity gradients. *Physics of Fluids* 7(6), 1438–1446.
- Habermann, C. and F. Kindermann (2007).

- Multidimensional spline interpolation: Theory and applications. *Computational Economics* 30, 153–169.
- Honein, A. E. and P. Moin (2004). Higher entropy conservation and numerical stability of compressible turbulence simulations. *Journal of Computational Physics* 201(2), 531–545.
- Kerimo, J. and S. S. Girimaji (2007). Boltzmann–BGK approach to simulating weakly compressible 3D turbulence: comparison between lattice Boltzmann and gas kinetic methods. *Journal of Turbulence* 8(46), 1–16.
- Kumar, G., S. S. Girimaji and J. Kerimo (2013). WENO-enhanced gas-kinetic scheme for direct simulations of compressible transition and turbulence. *Journal of Computational Physics* 234, 499–523.
- Liao, W., Y. Peng and L.-S. Luo (2009). Gas-kinetic schemes for direct numerical simulations of compressible homogeneous turbulence. *Physics Review E* 80(4), 046702.
- Liu, X. D., S. Osher and T. Chan (1994). Weighted essentially non-oscillatory schemes. *Journal of Computational Physics* 115(1), 200 – 212.
- Martín, M. P., E. M. Taylor, M. Wu and V. G. Weirs (2006). A bandwidth-optimized WENO scheme for the effective direct numerical simulation of compressible turbulence. *Journal of Computational Physics* 220(1), 270–289.
- Martin, M., E. Taylor, M. Wu and V. Weirs (2006). A bandwidth-optimized weno scheme for the effective direct numerical simulation of compressible turbulence. *Journal of Computational Physics* 220(1), 270 – 289.
- May, G., B. Srinivasan and A. Jameson (2007). An improved gas-kinetic BGK finite-volume method for three-dimensional transonic flow. *Journal of Computational Physics* 220(2), 856–878.
- Parashar, N., B. Srinivasan, S. S. Sinha and M. Agarwal (2017). Gpu-accelerated direct numerical simulations of decaying compressible turbulence employing a gkm-based solver. *International Journal for Numerical Methods in Fluids* 83(10), 737–754.
- Passot, T. and A. Pouquet (1987). Numerical simulation of compressible homogeneous flows in the turbulent regime. *Journal of Fluid Mechanics* 181, 441–466.
- Ragta, L. K., B. Srinivasan and S. S. Sinha (2017a). Efficient simulation of multidimensional continuum and non-continuum flows by a parallelised unified gas kinetic scheme solver. *International Journal of Computational Fluid Dynamics* 31(6-8), 292–309.
- Ragta, L. K., B. Srinivasan and S. S. Sinha (2017b). Unified gas kinetic scheme combined with cartesian grid method for intermediate mach numbers. *International Journal for Numerical Methods in Fluids* 85(9), 507–524.
- Samtaney, R., D. I. Pullin and B. Kosovic (2001). Direct numerical simulation of decaying compressible turbulence and shocklet statistics. *Physics Fluids* 13(5), 1415–1430.
- Sandham, N., Q. Li and H. Yee (2002). Entropy splitting for high-order numerical simulation of compressible turbulence. *Journal of Computational Physics* 178(2), 307 – 322.
- Sarkar, S., G. Erlebacher and M. Y. Hussaini (1991). Direct simulation of compressible turbulence in a shear flow. *Theoretical and Computational Fluid Dynamics* 2(5-6), 291–305.
- Xu, K. (1998). Gas-kinetic schemes for unsteady compressible flow simulations. Lecture series-van Karemman Institute for fluid dynamics 3, C1–C202.
- Xu, K. (2001). A gas-kinetic BGK scheme for the Navier–Stokes equations and its connection with artificial dissipation and Godunov method. *Journal of Computational Physics* 171(1), 289–335.
- Xu, K., M. Mao and L. Tang (2005). A multidimensional gas-kinetic BGK scheme for hypersonic viscous flow. *Journal of Computational Physics* 203(2), 405–421.
- Yeung, P. K. and S. B. Pope (1989). Lagrangian statistics from direct numerical simulations of isotropic turbulence. *Journal of Fluid Mechanics* 207, 531–586.